Homeotropic orientation of an ion-channel forming mesophase induced by nanotemplate wetting

Jaime J Hernandez, Denis V Anokhin, Martin Rosenthal, Xiaomin Zhu, Dimitri A Ivanov

ARTICLE

Homeotropic orientation of ion-channel forming mesophase induced by nanotemplate wetting

Received 00th January 20xx,
Accepted 00th January 20xx

DOI: 10.1039/x0xx00000x

Jaime J. Hernandez,*[a,§] Denis V. Anokhin,[b,c] Martin Rosenthal,[a,‖] Xiaomin Zhu[d] and Dimitri A. Ivanov*[a,b,c]

Anodic Aluminum Oxide (AAO) membranes were used as templates to control orientation of an ion-channel forming columnar mesophase obtained by self assembly of a wedge-shaped sulfonate molecule. Inside the AAO structure, the director vector of the mesophase is oriented parallel to the pore axis due to confinement effect. The molecular arrangement induced by the spatial confinement within the pores is extended over several microns into the remnant film on the AAO surface. The homeotropic alignment of the channels promotes unidimensional ion conduction through the film plane, which manifests as a considerable increase in conductivity relative to isotropic samples.

Introduction

Generation of supramolecular structures with different dimensionalities (1D-3D) through self-assembly has proven to be a powerful tool for designing materials with tailored properties.[1-2] The anisotropic physical characteristics of columnar mesophases have attracted considerable interest because of their potential use in various fields.[3-6] For a number of practical applications, it is desirable to achieve uniaxially oriented and highly ordered columnar superstructures on a macroscopic scale.[7-9] In-plane alignment is considered as thermodynamically more stable, however, for photovoltaic cells, light-emitting diodes (LEDs),[10-11] or ion-conducting membranes [12-15] metastable homeotropic alignment—with the columnar axis oriented perpendicular to the substrate or membrane plane—is necessary. Several factors affect the orientation of liquid crystals (LC) in open films; among others, the orientation can be correlated with the surface energy of the substrate and the chemical structure of the mesogen.[16-17] Interfacial interactions can play a central role in controlling molecular orientation through differences in surface tension between air/LC and LC/substrate interfaces.[18] Various approaches have been shown to be effective in achieving homeotropic alignment of columnar mesophases in open films, including tuning the surface energy, controlling annealing conditions based on film thickness, or using nanopatterned surfaces.[15, 19-24] One of the ways to achieve homeotropic alignment can be the use of porous nanotemplates for example based on anodic aluminum oxide (AAO).[25, 26] The AAO are formed by electrochemical anodization of aluminum wafers and consists of a parallel array of pores with pore axes well-ordered on a 2D plane, which makes the structure resembling a honeycomb. In addition, the pore diameter can be tailored in a wide range from 8 to 500 nm, depending on the anodization process conditions.[26] The use of AAO nanotemplates for structuring of functional materials helped improving the proton mobility and subsequently proton conductivity for proton exchange membranes [27], allowed to control orientations and ordering of conjugated polymers [28] and made it possible to obtain one-dimensional supramolecular wires of discotic molecules with the columnar axes uniformly oriented along pore axes on a macroscopic scale.[29]

In the present work, we focus on the supramolecular self-assembly of amphiphilic molecules bearing a sulfonate group at its focal point, which were previously shown to exhibit columnar structures with well-defined ion-conducting channels.[30-31] In particular, the studies have been carried out on a wedge-shaped sulfonate molecule, sodium 2,3,4-tris(11'-acryloylundecyl-1'-oxy)benzene-sulfonate (A-Na). Depending on temperature and relative humidity (RH) conditions, lamellar, columnar, or bicontinuous cubic phases, formed by self-assembly processes of A-Na, have been observed. At room temperature and low humidity conditions (RH < 55%), the studied wedge-shaped molecule forms a columnar hexagonal mesophase (Col_{hd}), where the sulfonate

[a] Institut de Sciences des Matériaux de Mulhouse (IS2M), CNRS UMR 7361, 15, rue Jean Starcky, F-68057 Mulhouse (France). E-mail: dimitri.ivanov@uha.fr
[b] Faculty of Chemistry, Lomonosov Moscow State University (MSU), GSP-1, 1-3 Leninskiye Gory, 119991 (Russian Federation).
[c] Scientific Center for Genetics and Life Sciences, Sirius University of Science and Technology, 1 Olympic Ave., 354340 Sochi, Russian Federation
[d] College of Textile Science and Engineering (International Institute of Silk), Zhejiang Sci-Tech University, Hangzhou 310018, China
[§] Present address: Madrid Institute for Advanced Studies in Nanoscience (IMDEA Nanoscience), Ciudad Universitaria de Cantoblanco, C/Faraday 9, Madrid 28049 (Spain).
[‖] Present address: Department of Chemistry, KU Leuven, Celestijnenlaan 200F, Box 2404, B-3001 Leuven (Belgium).

† Footnotes relating to the title and/or authors should appear here.
Electronic Supplementary Information (ESI) available: [details of any supplementary information available should be included here]. See DOI: 10.1039/x0xx00000x

groups are located on the column axis, giving rise to a well-defined ion-transporting channel.[32] The A-Na molecule presents an interesting example of a mesogen the structure of which can be arrested by photopolymerization [32-34]. The molecular structure of A-Na was inspired by the idea of Kato and colleagues of introducing polymerizable moieties into the chemical structure of the mesogen.[15] Photopolymerization was shown to produce mechanically stable materials suitable for membrane applications when the structure and orientation of the initial mesophase can be efficiently controlled.

Here, we demonstrate how nanoporous AAO templates can be used to achieve homeotropic alignment of the Col_{hd} mesophase formed by the A-Na sulfonate molecule on large areas of thick membranes (~ 80 µm thick). As it was shown, the orientation of the 1D-confined Col_{hd} phase inside the porous structure of the AAO is transmitted to the film deposited on top of the membrane, forcing the supramolecular columns to orient perpendicularly to the plane of the membrane.

Results and Discussion

Initially, the influence of the surface energy and topography on the morphology of the A-Na columnar mesophase on thin films was evaluated. The obtained results are summarized in Figure 1.

Three different substrates were employed: bared Si wafers, ITO coated glass slides (substrate with high surface energy) and PTFE-rubbed Si substrates, which, besides the low surface energy value, were used previously to induce homeotropic alignment of columnar phases.[24] Films with different thickness (tens to hundreds of nm) were prepared by spin-coating or solution casting over Si substrates. The morphology of the films was studied by means of Grazing Incidence X-ray Scattering (GIXS), which has been proved as a powerful technique for investigation of mesophases formed in thin films.[32-37] Fig. 1a shows the 2D X-ray patterns obtained from spin coated A-Na films over Si and ITO substrates. GIXS reveals the same highly oriented textures in both cases. The ratio between d-spacings was found to be 1:√3:2 which confirms the presence of a Col_{hd} phase. Miller indices of these reflections are indicated. The column diameter corresponding to the lattice parameter a=39.2 Å remains constant for all the samples. A characteristic 6-spot pattern on 2D-diffractogramm can be assigned to a planar alignment of the Col_{hd}, with the columnar axis lying parallel to the substrate, as schematically depicted in Fig. 1d. In the X-ray pattern corresponding to the film prepared over ITO, the refraction effects of the incidence beam due to the presence of ITO layer can be clearly observed in the meridian of the pattern.

In order to study the influence of the substrate topography thin films of A-Na were spin-coated over PTFE-rubbed substrates prepared as described in ref. [24]. In this case, the quality of the PTFE surface was confirmed by GIXS and Atomic Force microscopy (AFM) (see supporting info). Figure 1b-left shows a 2D pattern of the A-Na films spin coated over nanopatterned PTFE. The meridional peak located at wider angle corresponds to the d-spacing of 4.9 Å. This reflection indicates that the PTFE rubbed film has a hexagonal phase with a unit cell parameter a=5.7 Å, in good agreement with the data reported in the literature **[**38**]**.

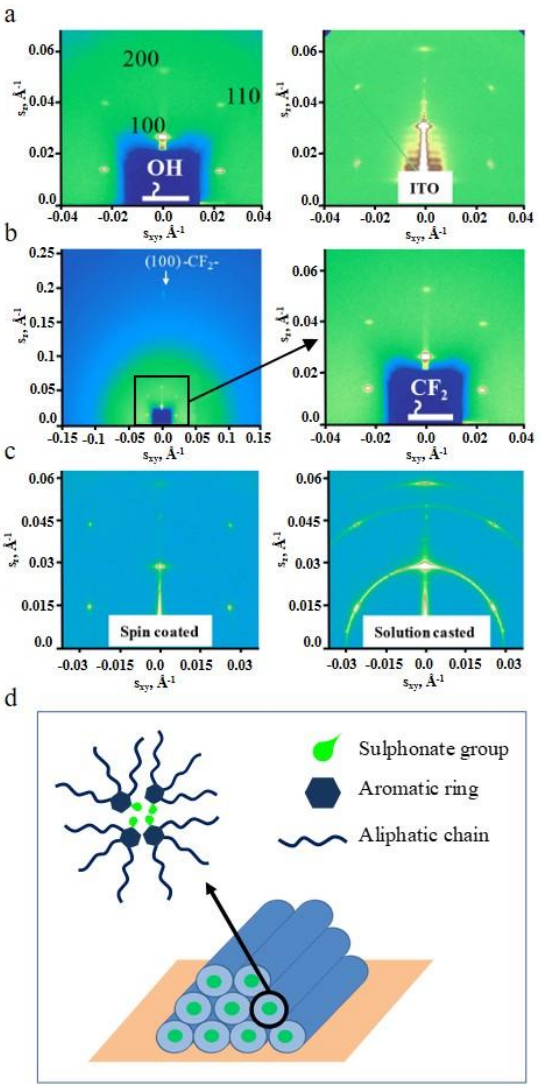

Figure 1. (a) 2D GIXS patterns of A-Na thin films spin-coated over Si (left) and ITO (right). The Miller indices of Col_{hd} phase are indicated. (b) 2D GIXS pattern of A-Na film prepared over PTFE-rubbed Si substrate. Reflection testifying the presence of PTFE is indicated in the meridian (left). Enlarged area showing peaks corresponding to the Col_{hd} phase is shown on the right. (c) 2D GIXS patterns of samples with different thickness. (d) Schematic view of the in plane alignment of hexagonal columnar phase. Self-assembly of A-Na results in tetramers that are in turn stacked on top of each other to form supramolecular cylinders.

The reflections corresponding to the A-Na Col_{hd} mesophase are located at smaller angles (Fig. 1b-right), showing the same d-spacings and angular distribution as the ones observed in previous samples.

Finally, the influence of film thickness and thermal treatments was also analysed. Fig. 1c allows comparing the GIXS patterns

corresponding to spin-coated and solution casted films, with different thicknesses. As can be observed, the in-plane orientation of the Col_{hd} phase is preserved on a thicker sample, even if the azimuthal broadening of the peaks indicates that the degree of orientation in this case is lower. Thermal treatments including annealing of the film above the isotropization point followed by slow cooling did not affect significantly the final morphology and the in-plane orientation of the columns (see Supporting Information).

According to the results obtained, the forces acting at the A-Na/air interface strongly favour the in-plane orientation of the mesophase over the homeotropic one: the in-plane orientation largely dominates, as was previously reported for different systems.[18,37,39]. In principle, this fact emphasizes the challenge of obtaining homeotropically aligned open films. nevertheless, it is possible to take advantage of this trend if a different approach is used.

Nanoporous materials, like AAO membranes, have shown to be an effective substrate to induce orientation of mesophases due to spatial confinement effects.[40-41] As pointed out by Steinhart et al., orientation due to confinement competes with orientation imposed by the surface interaction with the pore walls.[40] Due to the characteristics of our system, the "in-plane" orientation is expected to occur inside the pores. If so, on the one hand, we can overcome the mentioned problem of mixture of the two orientations. On the other hand, it is reasonable to assume that the confinement imposed by the pore walls will induce orientation of the Col_{hd} supramolecular structure formed by A-Na in register with the columns lying parallel to the pore axis.

Template wetting process was used to infiltrate AAO porous templates. Figure 2a shows a SEM image of the template.

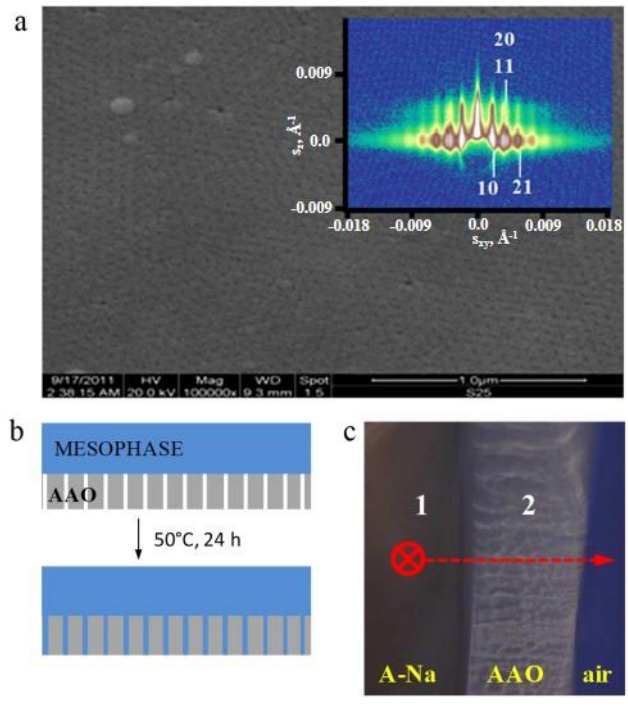

Figure 2. (a) SEM image of the 25nm pore size AAO template used in this work. Inset shows GISAXS pattern obtained at αi=0º. Reflections corresponding to the hexagonal packing of the pores are indicated. (b) Schematic view of the infiltration procedure of the AAO template. (c) Optical image of the cross section of the sample studied. Red dashed line indicates the scanning direction. Areas corresponding to the A-Na film, AAO membrane and air are indicated as 1 and 2 respectively.

Inset overlaid on the SEM image corresponds to the GIXS pattern obtained at αi=0º, with the X-ray beam parallel to the template plane. Several reflections corresponding to hexagonal arrangement of the pores in the template are indicated. A film of A-Na salt was blade coated by spreading a drop of the liquid crystal over the surface of the template. The sample was kept at 50 ºC, i.e. close to the isotropization temperature of the mesophase, under vacuum for 24 hours to favour complete filling of the membrane (Figure 2b).

Synchrotron X-ray microdiffraction was used for the structural characterization of the samples. The advantage of using small-sized beams to elucidate the structural changes due to the quasi-1D confinement realized inside the pores has been demonstrated.[38,42] An X-ray beam of 200 nm in diameter was used to scan along the cross section of the sample, with the beam parallel to the film surface (Fig. 2c). Diffraction patterns were collected at intervals of 1 µm allowing comparison of the structure and orientation of the mesophase in different regions of the sample, which are located outside, as well as inside the AAO template (cf. positions 1 and 2 in Fig. 2c, respectively). Figure 3a shows the corresponding 2D X-ray patterns. Amplifications of the low angle region are shown on the right for each case.

Radial integration using the whole angular region allows to obtain the 1D-reduced curve shown in Fig. 3b, where the scattering intensity is represented as a function of the norm of the scattering vector **s**. X-ray difractogram corresponding to the pattern obtained in region 1 displays five characteristic reflections at s=0.029, 0.049, 0.057, 0.075 and 0.085 Å $^{-1}$ (cf. Fig. 3b). The ratio of the corresponding d-spacings was found to be 1:√3:2:√7:3 which allowed assigning them to 10, 11, 20, 21 and 30 reflections of a 2D Col_{hd} lattice with columnar diameter **a** of 41.5Å, in good agreement with the values previously reported for thin films.[24]

At wider angles the presence of the characteristic halo due to stacking of the aliphatic chains is observed.[43] The structural parameters are the same inside the pores. The absorption of the sample generates the appearance of a sample image visible as a vertical shadow. The scattering intensity pertinent to the diffraction peaks is not homogeneously distributed along the diffraction circles, i.e. varies with the azimuthal angle. This reflects the existence of preferred orientation of the Col_{hd} mesophase along pore axis.

In order to evaluate the orientation of the columnar phase, a detailed study of the azimuthal distribution of scattered intensity was accomplished. The azimuthal intensity of the 10 reflection was represented as a function of the beam position during the scan (Figure 4a).

The interfaces AAO template/A-Na film and A-Na film/air are indicated on the figure with yellow and blue horizontal bars,

respectively. According to the scheme shown in Fig. 4b the meridional direction is located at azimuth angles of 90º and 270º.

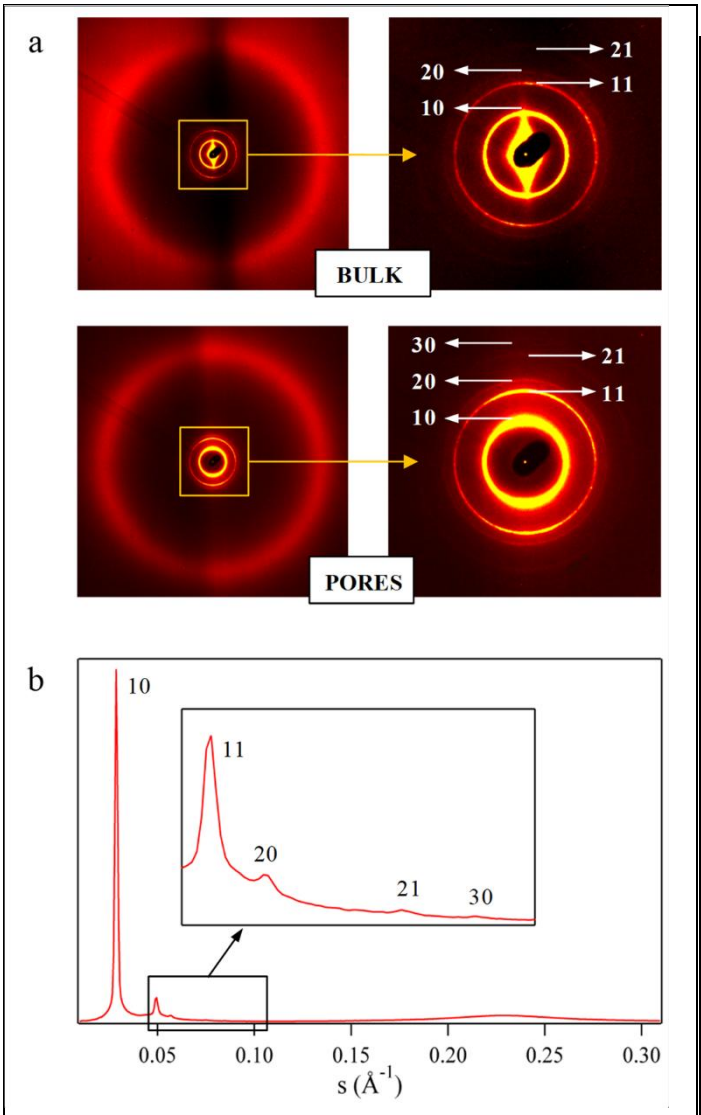

Figure 3. (a) 2D X-ray patterns corresponding to zones 1 and 2 indicated in Fig. 2c and amplification of medium angle regions in each case. (b) 1D-reduced scattering curve corresponding to region 1. The inset shows in detail the less intense peaks. Reflections corresponding to the Col_{hd} structure are indicated.

Although the scattered intensity coming from the infiltrated material is weaker than that generated by the remnant A-Na film, the existence of anisotropy can be clearly inferred from the azimuthal intensity distribution.

The Herman's orientation function (f_2) for uniaxially oriented systems defined as:

$$f_2 = \frac{1}{2}(3\langle cos^2\varphi\rangle - 1)$$

where φ is the angle between the azimuthal direction and reference axis. The f_2 function is commonly used to estimate the orientation of a sample from the analysis of wide or small-angle X-ray scattering data.[37,39]

In the present work, the Herman's orientation function was used to evaluate the columnar orientation of the mesophase. The s-range was adjusted for evaluation of the orientation of the 10 peak of the Col_{hd} phase. The directions of reference are

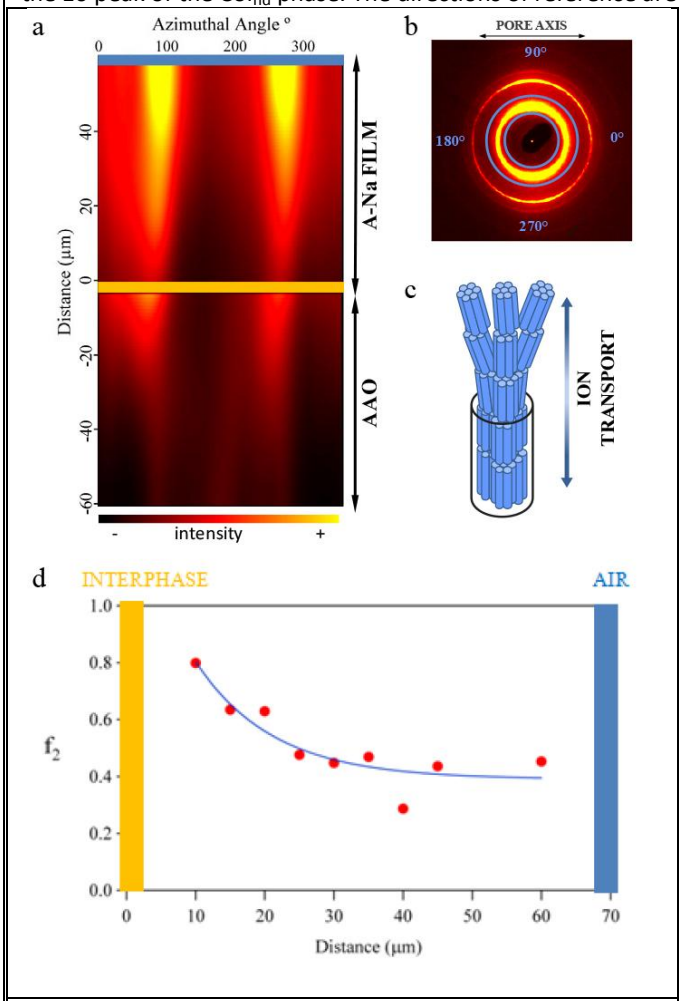

Figure 4. (a) Azimuthal intensity of the 10 reflection of the Col_{hd} phase as a function of position of the incident X-ray beam with respect to the membrane surface. Interfaces AAO template/A-Na film and A-Na film/air are indicated by yellow and blue horizontal bars, respectively. (b) 2D X-ray pattern indicating the region of interest (between blue rings) for the azimuthal integration corresponding to the 10 reflection as well as the reference angles used in the study. (c) Schematic view of the orientation of the columnar mesophase inside and outside the porous structure. The favoured ionic transport direction is indicated by the blue arrow. (d) Herman's orientation factor as a function of distance calculated for the A-Na film deposited over AAO template. The corresponding interfaces shown in (a) are indicated with vertical bars. Blue line is the fit of the experimental data with the exponential function.

indicated in Fig. 4b. For convenience, zero position for the calculation of f_2 was chosen at the meridian of the pattern (φ=90º), since the scattered intensity reaches maximum in this region. Prior to calculation of the f_2 function, the scattering curves were normalized after subtraction of the background. According to the chosen reference system, the orientation

function takes the value of 1 when the scattered intensity fully concentrates on the meridian and -0.5 when it concentrates on the equator. It is worth to mention that the scattering direction of the 10 reflection of the Col_{hd} structure is perpendicular to that of the columnar axis in the mesophase.

The measurements show that the columns are oriented parallel to the pore walls inside the AAO template, as it was expected. The unexpected fact is that the orientation of the columnar axis is preserved through the whole thickness of the remnant film, as schematically depicted in Fig. 4c. This means that the columns are oriented normal to the membrane surface in the entire membrane. The orientation function f_2 decays with the increase of the distance from the interface with the AAO template; the corresponding characteristic decay distance evaluated from the exponential fit equals 35 µm (Fig. 4d). Nevertheless, the value of f_2 remains higher than ca. 0.4 at the A-Na film/air interface, which is about 70 µm far away from the first interface. This emphasizes the importance of the 1D confinement inside the pores for the orientation of the surface film.

The existence of homeotropic orientation was independently confirmed by using polarized optical microscopy. A film of A-Na prepared as previously described was deposited on a glass cover. A reference sample was prepared substituting the AAO template by a second glass cover. Figure 5a shows the POM images obtained before and after the infiltration procedure for both systems. Initially, the same birefringence texture is observed (left images on each case). After the thermal treatment, the birefringence of the A-Na film sandwiched between glass covers seems to be improved. In the case of the sample prepared using the AAO template, the sample loses its birefringence and the corresponding POM image turns black when observed between crossed polarizers, indicating the formation of a homeotropically aligned columnar mesophase.[15,21,24] The degree of orientation of the Col_{hd} for each case is schematically shown on the insets.

It is important to note that, in some conditions, the organization of discotic liquid crystals can extend beyond simple uniaxial arrangements to include formations of circular concentric rings both perpendicular and parallel to the pore axis.[44-46] However, such structures lead to a significant increase in elastic energies because of the distortion of the 2D hexagonal column lattice at the curved pore surfaces. Consequently, the likelihood of these structures forming in small-sized pores, like those examined in this study, seems low.

Under these conditions, it is expected that unidirectional ionic transportation is favoured. In order to evaluate the effect of the orientation on the conductive properties of the material ion conductivity measurements were accomplished. Through-plane ion conductivity was measured at 25 °C by AC impedance spectroscopy at different relative humidity conditions (RH). Due to the high resistance of the AAO template, the opposite side to that in contact with the A-Na film was coated with gold to ensure electrical contact of the conductive paths formed through the porous with the ITO electrode. The reference sample was sandwiched between ITO coated glass slides. Schematic views of the cross-section of the setups used in each case are shown in Figure 5b.

Under dry conditions both samples show similar conductivities, in the range of 5.5 x 10^{-5} µS cm^{-1} (cf. Fig. 5c). In absence of water no conductivity is observed. This behaviour is similar to that observed for Nafion membranes, where presence of water is a requisite to reach high ion conductivity.[47-48] When RH increases up to 33%, a jump in the conductivity values is observed. While the reference sample reaches conductivity values of around 2.5x10^{-2} µS cm^{-1}, the A-Na film with ionic channels oriented perpendicular to its surface reaches 2.1x10^{-1} µS cm^{-1}, that is, almost one order of magnitude higher. The limited amount of conductive paths through the pores of the AAO template diminishes the effective contact area of the

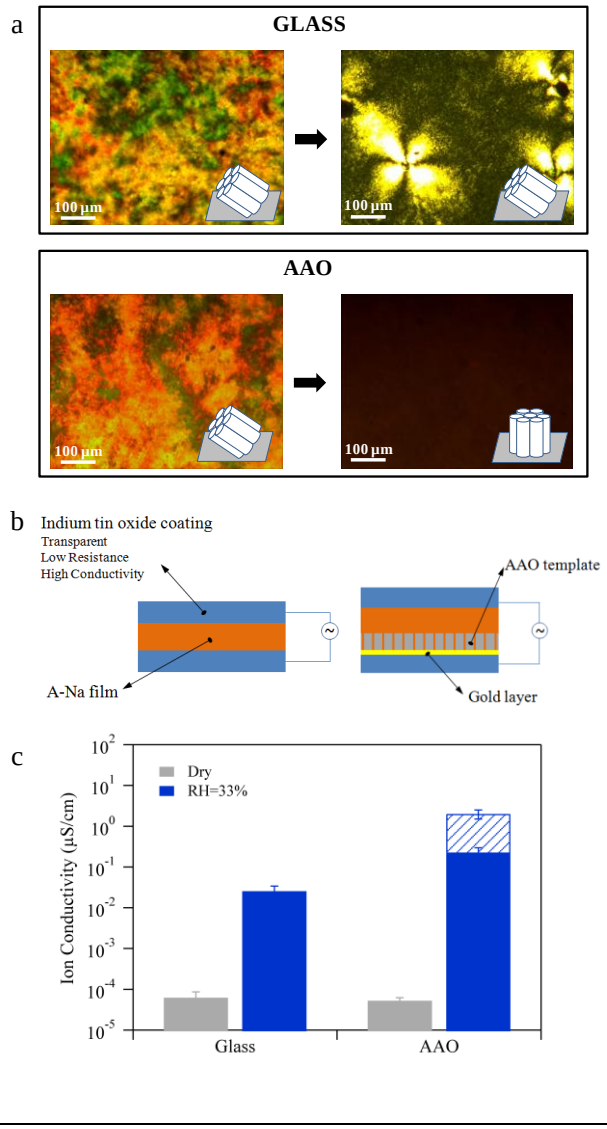

Figure 5. (a) POM images of A-Na films prepared between cover glasses (top) or using AAO template (bottom); before (left) and after (right) thermal treatment for the infiltration of the porous template. (b) Schematic view of the setup used to test the conductivity of the different samples prepared directly between ITO electrodes (left) or using

AAO templates (right). (c) Conductivity of samples prepared using different methods measured under dry conditions and at RH=33%. The value of conductivity extrapolated taking into account geometrical considerations is indicated with striped area.

electrode with the membrane. According to geometrical considerations, only about 10-12% of the membrane surface contributes to the measured value of conductivity. In this case, the total resistance of the sample can be considered then as the sum of the resistances of two layers: the aligned A-Na film and the infiltrated AAO template. According to our calculations, the real conductivity of the uniaxially oriented membrane is on the order of 10 μS cm^{-1}, that is, two orders of magnitude higher than the isotropic film value.

Conclusions

Orientation of an ion-channel forming columnar mesophase formed by self-assembly of a wedge-shaped sulfonate molecule was addressed for 1D-confinement within AAO membranes. The director vector of the mesophase was found to be oriented parallel to the pore axis inside the AAO structure. The molecular arrangement induced by the spatial confinement within the pores is extended over several microns into the remnant film on the AAO surface. The homeotropic alignment of the channels favours 1D ion conduction through the film providing a dramatic increase of the through-plane conductivity compared to that observed for isotropic samples which opens perspectives for self-assembled ionomeric materials with improved performance.

Experimental Section

Sample preparation: Si substrates (ITME, Institute of Electronic Materials Technology Warszawa, Poland) were cleaned using piranha solution (H_2SO_4:H_2O_2, 3:1) prior to use on each case. Highly oriented PTFE-rubbed surface was obtained with a home-built device by sliding a PTFE rod at 330°C at a speed of 0.6 $mm.s^{-1}$. AAO templates (Whatman, nominal pore size: 25 nm diameter, 60 μm thick) and ITO substrates (70-100 Ω/sq, Sigma-Aldrich) were cleaned by immersion in ultrasound bath with methanol for 30 minutes.

Thin films were prepared by spin-coating from A-Na solutions in $CHCl_3$ (20 mg ml^{-1}) over rotating substrates, applying a rotation speed of 2500 rpm during 45 s. In the case of solvent cast films, solution was deposited and slow solvent evaporation took place inside the lab hood.

Prior to conductivity measurements, the samples were annealed at 25 °C inside sealed vials under RH=33% using saturated solution of $MgCl_2$ for 60 h, and then measured under the same conditions. The so called "dry" sample was dried and kept under vacuum.

Sample characterization: GIXS measurements were accomplished at BW4 beamline at the Hamburger Synchrotronstrahlungslabor (HASYLAB) at Deutsches Elektronen-Synchrotron (DESY) (Hamburg, Germany) and X6B beamline at Brookhaven National Laboratory (BNL) (New York, EEUU). Wavelengths used were 1.38 and 0.68 Å, respectively. Incidence angles (α_i) of 0º or 0.4º were chosen, depending on the sample. 2D X-ray patterns were recorded using CCD detectors (marCCD165 and PI-SCX-4300, Princeton Instruments). The modulus of the scattering vector **s** was calculated using several diffraction orders of silver behenate.

Microfocus XRD experiments in transmission geometry were carried out at the ID13 beamline at the European Synchrotron Radiation Facility (ESRF) (Grenoble, France). The wavelength used was 0.81 Å. X-ray patterns were recorded by a two-dimensional CCD camera (FReLoN Kodak CCD). The sample-to-detector distance was calibrated by using a silver behenate standard.

Optical micrographs using polarized light were obtained by means of a LEITZ Laborlux 12 POL- S equipped with a digital camera DCM 310 with a C-mount.

Through-plane ion conductivity was measured at 25 °C by impedance spectroscopy using an Electrochemical Work-station IM6 (Zahner-Elektrik GmbH&Co. KG, Germany). The spectra were recorded with an amplitude of 1V in the frequency range from 100 to 10^8 Hz. The conductivity values were obtained by fitting the impedance spectra with a model containing a serial connection of a parallel and a serial RC-circuits.

Author Contributions

Conceptualisation and Supervision, D.A.I.; Data Curation and Writing- Original Draft, J.J.H.; Resources, X.Z.; Methodology, D.V.A.; Data Curation, M.R.

Conflicts of interest

There are no conflicts to declare.

Acknowledgements

D.V.A. acknowledge the Ministry of Science and Higher Education of the Russian Federation for financial support in the frame of state contract No 075-266 15-2022-1117 from June 30, 2022. The authors are grateful to the personnel of the BW4 beamline of HASYLAB at DESY and X6B beamline at Brookhaven National Laboratory (BNL). The authors acknowledge Dr. Emanuela Di Cola and Dr. Manfred Burghammer from the ID13 beamline of the ESRF (Grenoble) for fruitful discussions and excellent technical support.

Notes and references

1 B.-K. Cho, A. Jain, S. M. Gruner, U. Wiesner, Mesophase Structure-Mechanical and Ionic Transport Correlations in Extended Amphiphilic Dendrons. *Science*, 2004, **305(5690)**, 1598-1601.

2 R.A. Farrell, N. Petkov, M. A. Morris, J. D. Holmes, Self-assembled templates for the generation of arrays of 1-

dimensional nanostructures: From molecules to devices. *Journal of Colloid and Interface Science*, 2010, **349(2)**, 449-472.
3 B.R. Kaafarani, Discotic liquid crystals for opto-electronic applications. *Chemistry of Materials*, 2001, **23**, 18.
4 U. Beginn, G. Zipp, A. Mourran, P. Walther, M. Möller, Membranes Containing Oriented Supramolecular Transport Channels. *Advanced Materials*, 2000, **12(7)**, 513-516.
5 T. Kato, From Nanostructured Liquid Crystals to Polymer-Based Electrolytes. *Angewandte Chemie International Edition*, 2010, **49(43)**, 7847-7848.
6 C.-H. Ho, Y.-S. Lin, C.-C. Hung, Y.-C. Chiu, C.-C. Kuo, Y.-C. Lin, W.-C. Chen, Discotic Liquid Crystals with Highly Ordered Columnar Hexagonal Structure for Ultraviolet Light-Sensitive Phototransistor Memory. *ACS Applied Electronic Materials*, 2023, **5(2)**, 1067-1076.
7 H. Shimura, M. Yoshio, K. Hoshino, T. Mukai, H. Ohno, T. Kato, Noncovalent Approach to One-Dimensional Ion Conductors: Enhancement of Ionic Conductivities in Nanostructured Columnar Liquid Crystals. *Journal of the American Chemical Society*, 2008, **130(5)**, 1759-1765.
8 M. Yoshio, T. Mukai, H. Ohno, T. Kato, One-Dimensional Ion Transport in Self-Organized Columnar Ionic Liquids. *Journal of the American Chemical Society*, 2004, **126(4)**, 994-995.
9 Y. Huang, Y. Cong, J. Li, D. Wang, J. Zhang, L. Xu, W. Li, L. Li, G. Pana, C. Yang, Anisotropic ionic conductivities in lyotropic supramolecular liquid crystals. *Chemical Communications*, 2009, **48**, 7560-7562.
10 A. K. Yadav, B. Pradhan, H. Ulla, S. Nath, J. De, S. K. Pal, M. N. Satyanarayan, A. S. Achalkumar, Tuning the self-assembly and photophysical properties of bi-1,3,4-thiadiazole derivatives through electron donor-acceptor interactions and their application in OLEDs. *Journal of Materials Chemistry C*, 2017, **5(36)**, 9345 - 9358.
11 B. Mu, X. Hao, J. Chen, Q. Li, C. Zhang, D. Chen, Discotic columnar liquid-crystalline polymer semiconducting materials with high charge-carrier mobility via rational macromolecular engineering. *Polymer Chemistry*, 2017, **8(21)**, 3286 - 3293.
12 H. Shimura, M. Yoshio, A. Hamasaki, T. Mukai, H. Ohno, T. Kato, Electric-Field-Responsive Lithium-Ion Conductors of Propylenecarbonate-Based Columnar Liquid Crystals. *Advanced Materials*, 2009, **21(16)**, 1591-1594.
13 Charlet, E., et al., Ultrathin films of homeotropically aligned columnar liquid crystals on indium tin oxide electrodes. Applied Physics Letters, 2008. 92(2): p. 024107.
14 H.-S. Kim, S.-M. Choi, J.-H. Lee, P. Busch, S. J. Koza, E. A. Verploegen, B. D. Pate, Uniaxially Oriented, Highly Ordered, Large Area Columnar Superstructures of Discotic Supramolecules using Magnetic Field and Surface Interactions. *Advanced Materials*, 2008, **20(6)**, 1105-1109.
15 M. Yoshio, T. Kagata, K. Hoshino, T. Mukai, H. Ohno, T. Kato, One-Dimensional Ion-Conductive Polymer Films: Alignment and Fixation of Ionic Channels Formed by Self-Organization of Polymerizable Columnar Liquid Crystals. *Journal of the American Chemical Society*, 2006, **128(16)**, 5570-5577.
16 N. Boden, R. J. Bushby, P. S. Martin, S. D. Evans, R. W. Owens, D. A. Smith, Triphenylene-Based Discotic Liquid Crystals as Self-Assembled Monolayers. *Langmuir*, 1999, **15(11)**, 3790-3797.
17 N. Terasawa, H. Monobe, K. Kiyoharaa, Y. Shimizu, Strong tendency towards homeotropic alignment in a hexagonal columnar mesophase of fluoroalkylated triphenylenes. *Chemical Communications*, 2003, 1678-1679.
18 E. Grelet, H. Bock, Control of the orientation of thin open supported columnar liquid crystal films by the kinetics of growth. EPL (Europhysics Letters), 2006, **73(5)**, 712.
19 K. Perronet, F. Charra, Influence of molecular–substrate interaction on the self-assembly of discotic liquid crystals. *Surface Science*, 2004, **551(3)**, 213-218.
20 H.-T. Jung, S. O. Kim, Y. K. Ko, D. K. Yoon, S. D. Hudson, V. Percec, M. N. Holerca, W.-D. Cho, and P. E. Mosier, Surface Order in Thin Films of Self-Assembled Columnar Liquid Crystals. *Macromolecules*, 2002, **35(9)**, 3717-3721.
21 I. Cour, Z. Pan, L. T. Lebruin, M. A. Case, M. Furis, R. L. Headrick, Selective orientation of discotic films by interface nucleation. *Organic Electronics*, 2012, **13(3)**, 419-424.
22 T. D. Choudhury, N. V. S. Rao, R. Tenent, J. Blackburn, B. Gregg, I. I. Smalyukh, Homeotropic alignment and director structures in thin films of triphenylamine-based discotic liquid crystals controlled by supporting nanostructured substrates and surface confinement. Journal of Physical Chemistry B, 2011. 115: p. 9.
23 H.-G. Park, J.-J. Lee, K.-Y. Dong, B.-Y. Oh, Y.-H. Kim, H.-Y. Jeong, B.-K. Ju, D.-S. Seo, Homeotropic alignment of liquid crystals on a nano-patterned polyimide surface using nanoimprint lithography. Soft Matter, 2011, 7(12): p. 5610-5614.
24 R. I. Gearba, D. V. Anokhin, A. I. Bondar, W. Bras, M. Jahr, M. Lehmann, D. A. Ivanov, Homeotropic Alignment of Columnar Liquid Crystals in Open Films by Means of Surface Nanopatterning. *Advanced Materials*, 2007, **19(6)**, 815-820.
25 M. Steinhart, J. H. Wendorff, A. Greiner, R. B. Wehrspohn, K. Nielsch, J. Schilling, J. Choi, U. Gösele, Polymer nanotubes by wetting of ordered porous templates, *Science*, 2002, **296(5575)**, 1997.
26 J.T. Domagalski, E. Xifre-Perez, L.F. Marsal, Recent Advances in Nanoporous Anodic Alumina: Principles, Engineering, and Applications, *Nanomaterials*, 2021, **11**, 430.
27 X.H. Yan, H.R. Jiang, G. Zhao, L. Zeng, T.S. Zhao, *Journal of Power Sources* 2016, **326**, 466-475.
28 H. Park, H. Park, H. Ahn, W. Lee, J. Park, B.J. Kim, D. K. Yoon, *Chem. Mater*. 2023, **35**, 1355−1362.
29 H. Duran, B. Hartmann-Azanza, M. Steinhart, D. Gehrig, F. Laquai, X. Feng, K. Müllen, H.-J. Butt, G. Floudas. *ACS Nano* 2012, **6(11)**, 9359–9365.
30 X. Zhu, B. Tartsch, U. Beginn, M. Möller, Wedge-Shaped Molecules with a Sulfonate Group at the Tip—A New Class of Self-Assembling Amphiphiles. *Chemistry – A European Journal*, 2004, **10(16)**, 3871-3878.
31 X. Zhu, M. A. Scherbina, A. V. Bakirov, B. Gorzolnik, S. N. Chvalun, U. Beginn, M. Möller, Methacrylated Self-Organizing 2,3,4-Tris(alkoxy)benzenesulfonate: A New Concept Toward Ion-Selective Membranes. *Chemistry of Materials*, 2006, **18(19)**, 4667-4673.
32 H. Zhang, L. Li, M. Möller, X. Zhu, J. J. Hernandez Rueda, M. Rosenthal, D. A. Ivanov, *Advanced Materials* 2013, **25**, 3543-3548.
33 Y. Chen, M. D. Lingwood, M. Goswami, B. E. Kidd, J. J Hernandez, M. Rosenthal, D. A. Ivanov, J. Perlich, H. Zhang, X. Zhu, M. Möller, L. A. Madsen, *Journal of Physical Chemistry B,* 2014, **118**, 3207–3217.
34 J. J Hernandez, H. Zhang, M. Rosenthal, M. D. Lingwood, M. Goswami, Y. Chen, X. Zhu, M. Möller, L. Madsen, D. A. Ivanov, *Macromolecules* 2017, **50(14)**, 5392–5401.
35 D. R Rueda, A. Nogales, J. J Hernandez, M.-C. García-Gutiérrez, T. A. Ezquerra, S. V Roth, M. G Zolotukhin, R. Serna, Stacking of Main Chain-Crown Ether Polymers in Thin Films. *Langmuir*, 2007, **23(25)**, 12677-12681.
36 G. Ungar, F. Liu, X. B. Zeng, B. Glettner, M. Prehm, R. Kieffer, C. Tschierske, GISAXS in the study of supramolecular and hybrid liquid crystals. *Journal of Physics: Conference Series*, 2010, **247(1)**, 012032.
37 A. M. Hiszpanski, S. S. Lee, H. Wang, A. R. Woll, C. Nuckolls, Y.-L. Loo, Post-deposition Processing Methods To Induce

Preferential Orientation in Contorted Hexabenzocoronene Thin Films. *ACS Nano*, 2012, **7(1)**, 294-300.

38 Y. Odarchenko, M. Defaux, M. Rosenthal, A. Akhkiamova, P. Bovsunovskaya, A. Melnikov, A. Rodygin, A. Rychkov, K. Gerasimov, D.V. Anokhin, X. Zhu, D.A. Ivanov, One Methylene Group in the Side Chain Can Alter by 90 Degrees the Orientation of a Main-Chain Liquid Crystal on a Unidirectional Substrate, *ACS Macro Lett*. 2018, **7**, 453−458.

39 C. Hong, T.-T. Tang, C.-Y. Hung, R.-P. Pan, W. Fang, Liquid crystal alignment in nanoporous anodic aluminum oxide layer for LCD panel applications. *Nanotechnology*, 2010, **21(28)**, 285201.

40 M. Steinhart, S. Zimmermann, P. Göring, A. K. Schaper, U. Gösele, C. Weder, J. H. Wendorff, Liquid Crystalline Nanowires in Porous Alumina: Geometric Confinement versus Influence of Pore Walls. *Nano Letters*, 2004, **5(3)**, 429-434.

41 M.-C. García-Gutiérrez, A. Linares, J. J. Hernández, D. R. Rueda, T. A. Ezquerra, P. Poza, R. J. Davies, Confinement-Induced One-Dimensional Ferroelectric Polymer Arrays. *Nano Letters*, 2010, **10(4)**, 1472-1476.

42 M. C. García-Gutiérrez, J. J. Hernández, A. Nogales, P. Panine, D. R. Rueda, and T. A. Ezquerra, Influence of Shear on the Templated Crystallization of Poly(butylene terephthalate)/Single Wall Carbon Nanotube Nanocomposites. *Macromolecules*, 2008, **41(3)**, 844-851.

43 X. Zhu, U. Beginn, M. Möller, R.I. Gearba, D.V. Anokhin, D.A. Ivanov, Self-Organization of Polybases Neutralized with Wedge-Shaped Sulfonic Acid Molecules – a New Approach towards Supramolecular Cylinders*, Journal of the American Chemical Society*, 2006, **128**, 16928-16937.

44 Z. Li, A. R. Raab, M. A. Kolmangadi, M. Busch, M. Grunwald, F. Demel, F. Bertram, A. V., Kityk, A. Schönhals, S. Laschat, P. Huber, How do ionic superdiscs self-assemble in nanopores? arXiv:2401.12663v1

45 K. Sentker, A. Yildirim, M. Lippmann, A. W. Zantop, F. Bertram, T. Hofmann, O. H. Seeck, A. V. Kityk, Self-assembly of liquid crystals in nanoporous solids for adaptive photonic metamaterials, *Nanoscale*, 2019, **11**, 23304–23317.

46 K. Sentker, A. W. Zantop, M. Lippmann, T. Hofmann, O. H. Seeck, Andriy V. Kityk, A. Yildirim, A. Schönhals, M. G. Mazza, P. Huber, *Physical Review Letters* 2018, **120**, 067801.

47 P. Choi, N. H. Jalani, R. Datta, Thermodynamics and Proton Transport in Nafion II. Proton Diffusion Mechanisms and Conductivity. *Journal of The Electrochemical Society*, 2005, **152(3)**, E123-E130.

48 T. A. Zawodzinski Jr., C. Derouin, S. Radzinski, R. J. Sherman, V. T. Smith, T. E. Springer, S. Gottesfeld, Water Uptake by and Transport Through Nafion® 117 Membranes. *Journal of The Electrochemical Society*, 1993, **140(4)**, 1041-1047.